Checkerboard Julia Sets for Rational Maps

Paul Blanchard
Figen Çilingir*
Daniel Cuzzocreo
Robert L. Devaney
Daniel M. Look
Elizabeth D. Russell

Current version: June 16, 2011
Original draft: February 8, 2010

Abstract. In this paper, we consider the family of rational maps

$$F_\lambda(z) = z^n + \frac{\lambda}{z^d},$$

where $n \geq 2$, $d \geq 1$, and $\lambda \in \mathbb{C}$. We consider the case where λ lies in the main cardioid of one of the $n - 1$ principal Mandelbrot sets in these families. We show that the Julia sets of these maps are always homeomorphic. However, two such maps F_λ and F_μ are conjugate on these Julia sets only if the parameters at the centers of the given cardioids satisfy $\mu = \nu^{j(d+1)}\lambda$ or $\mu = \nu^{j(d+1)}\overline{\lambda}$ where $j \in \mathbb{Z}$ and ν is an $n - 1^{\text{st}}$ root of unity. We define a dynamical invariant, which we call the minimal rotation number. It determines which of these maps are conjugate on their Julia sets, and we obtain an exact count of the number of distinct conjugacy classes of maps drawn from these main cardioids.

In recent years there have been many papers dealing with the family of rational maps given by

$$F_\lambda(z) = z^n + \frac{\lambda}{z^d},$$

where $n \geq 2$, $d \geq 1$, and $\lambda \in \mathbb{C}$ [9]. For many parameter values, the Julia sets for these maps are Sierpiński curves, i.e., planar sets that are homeomorphic to the well-known Sierpiński carpet fractal. One distinguishing property of Sierpiński curve Julia sets is that the Fatou set consists of infinitely many open disks, each bounded by a simple closed curve, but no two of these bounding curves intersect.

There are many different ways in which these Sierpiński curves arise as Julia sets in these families. For example, the Julia set is a Sierpiński curve if λ is a parameter for which

1. the critical orbits enter the immediate basin of attraction of ∞ after two or more iterations [5];

2. the parameter lies in the main cardioid of a "buried" baby Mandelbrot set [3]; or

3. the parameter lies on a buried point in a Cantor necklace in the parameter plane [7].

The parameter planes for these maps in the cases where $n = d = 3$ and $n = d = 4$ are shown in Figure 1. The red disks not centered at the origin are regions where the first case above occurs. These disks are called Sierpiński holes.

Many Mandelbrot sets are visible in Figure 1. The ones that touch the external red region are not "buried," so their main cardioids do not contain Sierpiński curve Julia sets. Only the ones that do not meet this boundary contain parameters from case 2.

Finally, numerous Cantor necklaces, i.e., sets homeomorphic to the Cantor middle-thirds set with the removed open intervals replaced by open disks, appear in these figures. The buried points in the Cantor set portion of the necklace are the parameters for which case 3 occurs.
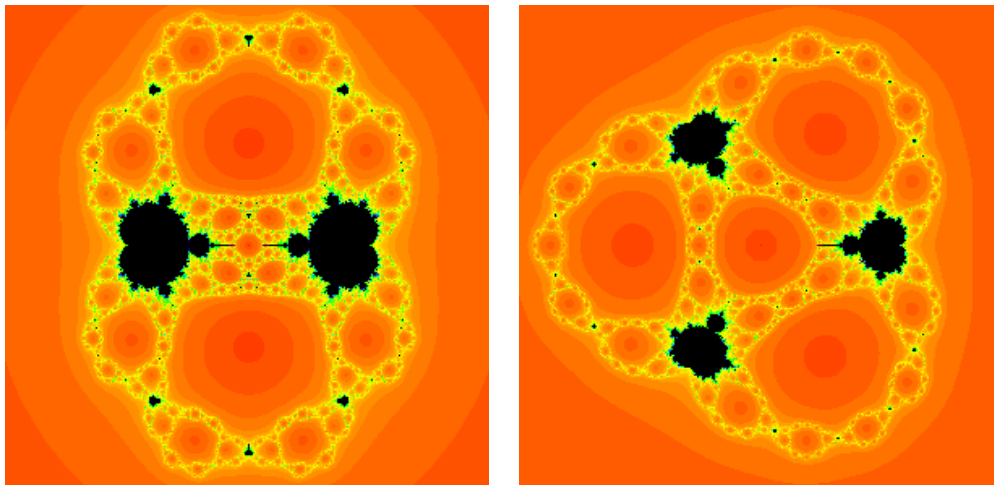
Figure 1: Two parameter planes: $n = d = 3$ (left) and $n = d = 4$ (right).

The dynamical behavior on Sierpiński curve Julia sets drawn from non-symmetrically located Sierpiński holes is never the same [6]. That is, only symmetrically located Sierpiński holes contain parameters for which the corresponding maps have conjugate dynamics. While it is known that two such maps are not conjugate on their Julia sets, there is no known dynamical invariant that explains this lack of conjugacy.

In this paper, we describe the topology of and dynamics on a very different type of Julia set that arises in these families, the "checkerboard" Julia sets. The parameter spaces contain $n - 1$ "principle Mandelbrot sets," the largest Mandelbrot sets in the parameter space [8]. We consider the Julia sets for the parameters that lie in the main cardioids of these Mandelbrot sets.

Parameters from these cardioids have two distinct types of Fatou components (see Figure 2). Since ∞ is a superattracting fixed point, the immediate basin of ∞ and its preimages lie in the Fatou set. These components are the escaping Fatou components. The Fatou set also contains a collection of components corresponding to other finite attracting periodic orbits and their preimages. These components are the non-escaping Fatou components. As we shall show, none of the boundaries of the escaping Fatou components

intersect. Likewise, the boundaries of the non-escaping Fatou components do not intersect. However, each such boundary intersects infinitely many boundaries of the escaping Fatou components, and each boundary of an escaping Fatou component intersects infinitely many non-escaping boundaries. Hence, the topology of these Julia sets is very different from the topology of Sierpiński curve Julia sets. We use the word "checkerboard" to describe this pattern of Fatou components.

In Figure 2, we display the Julia set for the map $F_{0.18}(z) = z^4 + 0.18/z^3$. The red regions are the preimages of the attracting basin of ∞, and the black regions are the preimages of the basins of the finite attracting cycles. The boundary of each red region touches infinitely many boundaries of the black regions, but it does not touch the boundary of any other red region. Similarly, the boundary of each black region touches infinitely many boundaries of the red regions, but it does not touch the boundary of any other black region.
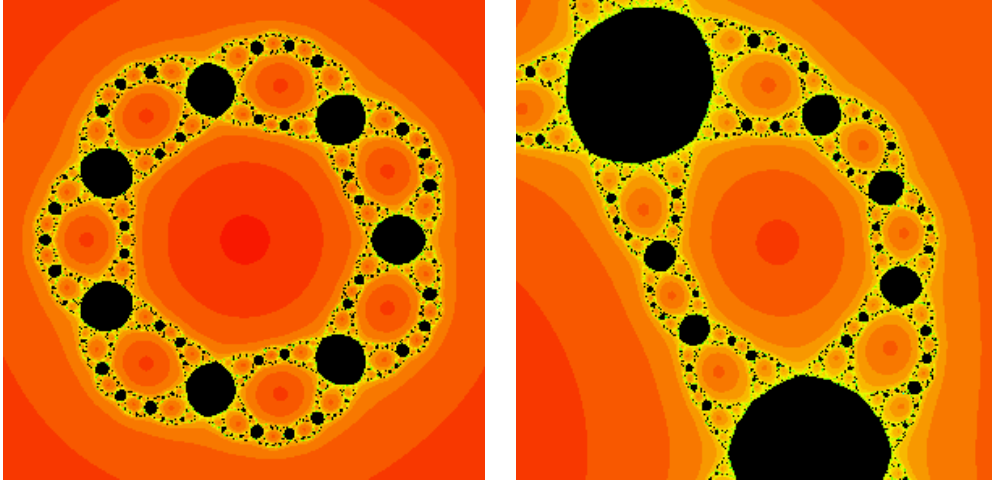

Figure 2: The image on the left is the checkerboard Julia set for $F_{0.18}(z) = z^4 + 0.18/z^3$. The image on the right is a magnification of one-seventh of the Julia set.

The external red region in the left-hand image of Figure 2 is the immediate basin of attraction of ∞. We denote this basin by B_λ. The central red region

3

that contains the pole at the origin is mapped to B_λ. We let T_λ denote this Fatou component. All other red regions are also eventually mapped to B_λ.

Note that there are $n + d$ ($= 7$ in this example) large black regions that touch B_λ and T_λ at unique points. These Fatou components are (eventually) periodic. We call them the connecting (Fatou) components since they are the only Fatou components that extend from B_λ to T_λ. Each of these connecting components seems to be separated by another red region that touches exactly two boundaries of the adjacent connecting components. On one side of these red regions, we see $d-1$ ($= 2$ in this example) smaller black components. On the other side, we see $n-1$ ($= 3$ in this example) smaller black components. Each such black component connects to a pair of red regions. If we were to magnify this image, we would see that this pattern repeats itself at any scale.

In this paper, we make this construction precise. In particular, we give an algorithm for describing the topological structure of these Julia sets. This algorithm also describes the dynamics on these Julia sets via symbolic dynamics. We prove:

Theorem 1. *Let $F_\lambda(z) = z^n + \lambda/z^d$ with $n \geq 2$ and $d \geq 1$. Any two Julia sets that correspond to parameters in the main cardioids of the principal Mandelbrot sets in the parameter plane for these maps are homeomorphic.*

Theorem 1 says that checkerboard Julia sets are analogous to Sierpiǹski curve Julia sets [15] because all checkboard Julia sets are homeomorphic.

As in the Sierpiǹski case [6], only certain symmetrically located cardioids give rise to conjugacies on their respective Julia sets. However, unlike the Sierpiǹski case, we can define a dynamical invariant for checkboard Julia sets. We call it the minimal rotation number, and we prove that it is a conjugacy invariant for checkerboard Julia sets.

Theorem 2. *Two maps drawn from different main cardioids of principal Mandelbrot sets are topologically conjugate on their Julia sets if and only if their minimal rotation numbers are equal. In particular, two such maps restricted to their Julia sets are topologically conjugate only if the parameters*

4

are symmetric either under the rotation $z \mapsto \nu^{j(d+1)} z$ or under the map $z \mapsto \nu^{j(d+1)} \overline{z}$, where $j \in \mathbb{Z}$ and $\nu^{n-1} = 1$.

Theorem 2 leads to an exact count of the number of main cardioids that have non-conjugate dynamics.

Theorem 3. *Let g be the greatest common divisor of $n - 1$ and $n + d$. If g is even, then there are exactly $1 + g/2$ distinct conjugacy classes among the maps drawn from the main cardioids of the principal Mandelbrot sets. If g is odd, then the number of conjugacy classes is $(g + 1)/2$.*

1   Preliminaries

Consider the family of maps

$$F_\lambda(z) = z^n + \frac{\lambda}{z^d}$$

where $n \geq 2$, $d \geq 1$, and $\lambda \in \mathbb{C}$. The point at infinity is superattracting of order n. As above, we denote the immediate basin of ∞ by B_λ. Also, 0 is a pole of order d, so there is a neighborhood of 0 that is mapped into B_λ. If this neighborhood is disjoint from B_λ, we use the term "trap door" for the preimage of B_λ that contains 0. We denote the trap door by T_λ.

The map $F_\lambda(z)$ has $n + d$ "free" critical points. They satisfy the equation

$$z^{n+d} = \frac{d\lambda}{n}.$$

Hence, they are equally spaced on the circle of radius

$$\sqrt[n+d]{\frac{d|\lambda|}{n}}$$

centered at the origin. There are also $n + d$ prepoles. They satisfy the equation $z^{n+d} = -\lambda$.

The family F_λ has symmetries in both the dynamical plane and the parameter plane.

Symmetry Lemma 1. *The map F_λ is conjugate to $F_{\bar\lambda}$ by the conjugacy $z \mapsto \bar z$.*

This first symmetry implies that the parameter plane is symmetric under complex conjugation.

Symmetry Lemma 2. *If ω is a $(n+d)$th root of unity, then*

$$F_\lambda(\omega z) = \omega^n F_\lambda(z).$$

This second symmetry implies that the Julia set of F_λ is symmetric under the map $z \mapsto \omega z$. Similarly, B_λ and T_λ possess this $(n+d)$-fold symmetry.

Moreover, since the free critical points are arranged symmetrically with respect to $z \mapsto \omega z$, all of the free critical orbits behave symmetrically with respect to this rotation. However, it is not necessarily true that all of these critical orbits behave in the same manner. For example, consider the map $F_{0.18}(z) = z^4 + 0.18/z^3$ (see Figure 2). The orbit of the free critical point on the positive real axis is asymptotic to a fixed point, but the other six free critical orbits are asymptotic to a pair of period-three orbits. This symmetry also implies that the basins of these attracting orbits are arranged symmetrically as well.

The most important consequence of Symmetry Lemma 2 is the fact that the orbits of all of the free critical points can be determined from the orbit of any one of them (see Figure 3). So the one-dimensional λ-plane is a natural parameter plane for these maps.

Symmetry Lemma 3. *Suppose that η is an $(n+d)(n-1)$st root of unity. Let $\nu = \eta^{n+d}$ and $\omega = \eta^{n-1}$. Then*

$$F_{\nu\lambda}^k(\eta z) = \eta^{n^k} F_\lambda^k(z)$$

for $k = 1,\ 2,\ 3,\ldots$.

Note that ν is an $(n-1)$st root of unity and ω is an $(n+d)$th root of unity. Symmetry Lemma 3 is proved by induction on k.
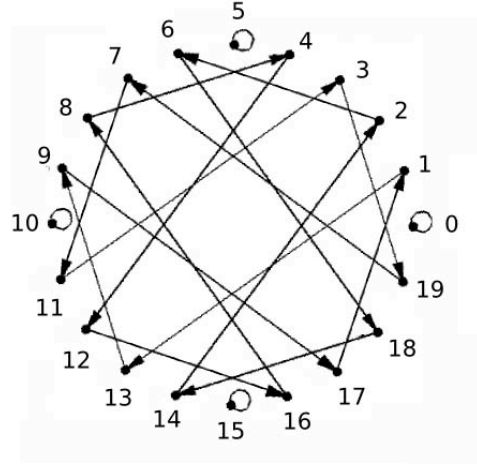
Figure 3: The orbit diagram for the critical points of $F_{\lambda_0}(z) = z^{13} + \lambda_0/z^7$ where λ_0 is the center of the principal Mandelbrot set $\mathcal{M}_0$ that intersects the positive real axis. The critical point on the positive real axis is a fixed point, and it is labeled with the number 0. The orbits of the remaining critical points are determined from the orbit of the fixed point using Symmetry Lemma 2.

We can determine the orbit diagram of $F_{\nu\lambda}$ from the orbit diagram of λ. In particular, if c_λ is a critical point for F_λ, then ηc_λ is a critical point for $F_{\nu\lambda}$. We denote this critical point by $c_{\nu\lambda}$. From Symmetry Lemma 3, we have

$$F_{\nu\lambda}^k (c_{\nu\lambda}) = F_{\nu\lambda}^k (\eta c_\lambda) = \eta^{n^k} F_\lambda^k (c_\lambda).$$

Therefore, the orbits of the critical points of F_λ and $F_{\nu\lambda}$ behave symmetrically with respect to rotation by some power of η (see Figure 4). Consequently, the parameter plane is symmetric under the rotation $\lambda \mapsto \nu\lambda$.

As we shall see, the dynamics of F_λ and $F_{\nu\lambda}$ are not necessarily conjugate. For example, if λ lies in the main cardioid of the right-hand principal Mandelbrot set in the $n = d = 3$ case, the map F_λ has a pair of attracting fixed points (see Figure 1). In contrast, if λ is an element of the the main cardioid of the left-hand principal Mandelbrot set, the map F_λ has an attracting cycle of period two.
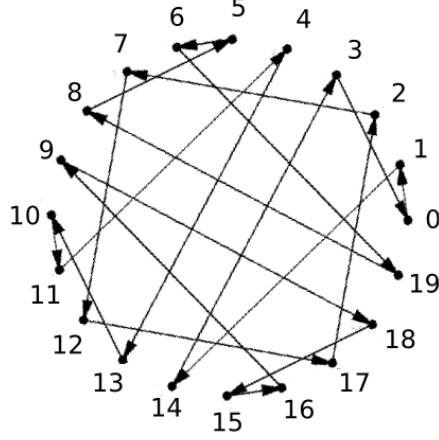
Figure 4: The orbit diagram for the critical points of $F_{\lambda_1}(z) = z^{13} + \lambda_1/z^7$ where $\lambda_1 = \nu\lambda_0$ is the center of the principal Mandelbrot set $\mathcal{M}_1$, i.e., the image of $\mathcal{M}_0$ under the rotation $z \mapsto \nu z$.

The map $F_{\nu\lambda}$ is conjugate to ωF_λ by the rotation $z \mapsto \eta z$ because

$$F_{\nu\lambda}(\eta z) = (\eta z)^n + \frac{\nu\lambda}{(\eta z)^d} = \eta^n z^n + \frac{\nu}{\eta^d}\frac{\lambda}{z^d} = \eta^n\left(z^n + \frac{\lambda}{z^d}\right) = \eta\omega\left(z^n + \frac{\lambda}{z^d}\right).$$

More generally, the map $F_{\nu^j\lambda}$ is conjugate to the map $\omega^j F_\lambda$ via the rotation $z \mapsto \eta^j z$.

As in the case of the quadratic polynomials $z^2 + c$, the orbits of the free critical points can tend to ∞. However, unlike the quadratic case, there are three distinct ways that these critical orbits can escape, and each way leads to a different topological type of Julia set.

Theorem (The Escape Trichotomy [5].) *Let $v_\lambda = F_\lambda(c_\lambda)$ be a critical value.*

1. *If v_λ lies in B_λ, then $J(F_\lambda)$ is a Cantor set.*

2. *If $T_\lambda \neq B_\lambda$ and v_λ lies in T_λ, then $J(F_\lambda)$ is a Cantor set of disjoint, simple, closed curves that surround the origin.*

8

3. In all other cases, $J(F_\lambda)$ is a connected set. In particular, if $T_\lambda \neq B_\lambda$ and $F_\lambda^j(v_\lambda)$ lies in T_λ for some $j \geq 1$, then $J(F_\lambda)$ is a Sierpiński curve.

We remark that case 2 of this theorem does not occur if $n = d = 2$ or if $d = 1$. In each parameter plane in Figure 1, the exterior red region consists of the parameters for which the Julia set is a Cantor set. We call this region the *Cantor set locus*. The small red region that contains the origin is the set of parameters for which the Julia set is a Cantor set of circles. We call this region the *McMullen domain* because McMullen first discovered this type of Julia set [12]. The complement of these two regions is the *connectedness locus*. The Julia sets for these parameters are connected. The "holes" in the connectedness locus consist of parameter values for which the Julia set is a Sierpiński curve. We call these regions *Sierpiński holes*.

Note that there are two large Mandelbrot sets along the real axis in the left parameter plane in Figure 1. In the right parameter plane in the same figure, there are three large Mandelbrot sets symmetrically located with respect to the rotation $z \mapsto \nu z$ where $\nu = e^{2\pi i/3}$.

With the exception of the $n = d = 2$ case, the parameter plane for the family F_λ contains $n - 1$ symmetrically located Mandelbrot sets if $d \neq 1$ [8]. We call these sets the principal Mandelbrot sets for the family F_λ. In [8], the existence of these sets was proved for the case $n = d > 2$. However, the same proof works if $d \neq 1$ and $n \neq d$. In this paper, we describe the structure of and dynamics on the Julia sets for parameters that lie in the main cardioids of these principal Mandelbrot sets.

If $n = d = 2$, there does not exist a principal Mandelbrot set in the parameter plane. In this case, the "tail" of the Mandelbrot set, i.e., the parameter corresponding to $c = -2$ in the Mandelbrot set for $z^2 + c$, extends to the origin, where the map is just $F_0(z) = z^2$. So, we do not have a complete Mandelbrot set. Nonetheless, there is a main cardioid in which each parameter has four connecting Fatou components (see the left-hand parameter plane in Figure 5).

If $d = 1$, there are no principal Mandelbrot sets in the parameter plane. However, there are $n - 1$ distinct cardioid-shaped regions extending from

the Cantor set locus to the origin (see the right-hand parameter plane in Figure 5). Parameters drawn from these regions have $n+1$ connecting Fatou components.
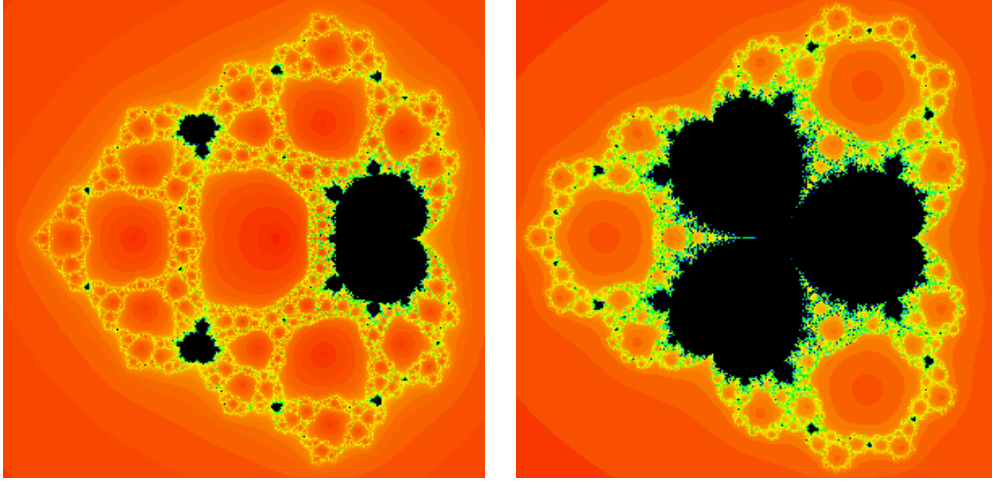

Figure 5: Two parameter planes: $n = d = 2$ (left) and $n = 4$, $d = 1$ (right).

For the maps that we study, the boundary of the immediate basin of infinity is a simple, closed curve.

Proposition 1. *Suppose λ lies in the connectedness locus in the parameter plane and F_λ is hyperbolic on its Julia set. Then the boundary of B_λ is a simple, closed curve.*

Proof: Since F_λ is hyperbolic on its Julia set, $J(F_\lambda)$ is locally connected (see [13]). In particular, the boundary of $J(F_\lambda)$ is locally connected, so ∂B_λ is a locally connected set. We need only show that the set $\overline{\mathbb{C}} - \overline{B_\lambda}$ is connected.

We argue by contradiction. Suppose that $\overline{\mathbb{C}} - \overline{B_\lambda}$ is disconnected. Let W_0 denote its component that contains the trap door. The second symmetry lemma implies that W_0 is symmetric under $z \mapsto \omega z$. Also, $\overline{T_\lambda}$ is contained in the interior of W_0 since, if not, there would be a critical point in $\partial T_\lambda \cap \partial B_\lambda$, which contradicts the assumption that F_λ is hyperbolic on $J(F_\lambda)$.

At least one other component of $\overline{\mathbb{C}} - \overline{B_\lambda}$, say W_1, is mapped over W_0. If not, ∂W_0 would be backward invariant, which cannot happen. Another

application of the second symmetry implies that $W_j = \omega^j W_1$ is also mapped onto W_0 for $j = 1, \ldots, n + d - 1$. We have $n + d$ distinct preimages of W_0.

However, we claim that there are points in W_0 that are also mapped into W_0. To see why, recall that ∂T_λ is mapped over the entire boundary of B_λ by F_λ and that ∂T_λ lies in W_0. Thus there is a point z_0 in ∂T_λ that is mapped into ∂W_0. Then there is a neighborhood of z_0 in W_0 mapped to a neighborhood of $F_\lambda(z_0)$, and hence there are points in this neighborhood that are mapped inside W_0. We arrive at a contradiction since we have found points in W_0 that have more than $n + d$ preimages.

$\square$

2   Checkerboard Julia Sets

In this section we present an algorithm for constructing the Julia sets for parameters in the main cardioids of the principal Mandelbrot sets. Theorem 1 follows from this algorithm.

First, consider the case of the principal Mandelbrot set whose main cardioid intersects the positive real axis, and let $[a, b]$ denote the interval of intersection. By considering the graph of $F_\lambda \,|\, \mathbb{R}$ for $\lambda \in (a, b)$, we see that each such map has an attracting fixed point that is real and positive. Hence, for each λ from this main cardioid, the map F_λ also has an attracting fixed point. We denote this fixed point by p_λ^0 and its immediate basin of attraction by C_λ^0. Since F_λ is hyperbolic, ∂C_λ^0 is a simple, closed curve. Furthermore, if $\lambda \in (a, b)$, the graph of $F_\lambda \,|\, \mathbb{R}$ shows that C_λ^0 extends from ∂B_λ to ∂T_λ. Consequently, C_λ^0 extends from ∂B_λ to ∂T_λ for all values of λ in this main cardioid. The intersection $\partial B_\lambda \cap \partial C_\lambda^0$ consists solely of a repelling fixed point q_λ^0 that is real and positive. Similarly, the intersection $\partial T_\lambda \cap \partial C_\lambda^0$ is also just one point that is real and positive. We denote it by u_λ^0. Note that $F_\lambda(u_\lambda^0) = q_\lambda^0$.

From the second symmetry, we obtain $n + d - 1$ other Fatou components that are symmetrically located around the origin. We denote these Fatou components by C_λ^j with $j = 1, \ldots, n + d - 1$. They are ordered in the coun-

terclockwise direction. Since each of these components extends from T_λ to B_λ, we call them *connecting (Fatou) components*. Some of these Fatou components are immediate basins of attracting cycles, and others are eventually periodic components. The exact configuration of these components is determined by Symmetry Lemma 2 with $\omega = \exp(2\pi i/(n+d))$. For example, since $F_\lambda(\omega z) = \omega^n F_\lambda(z)$, we have $F_\lambda(C_\lambda^1) = C_\lambda^n$, $F_\lambda(C_\lambda^2) = C_\lambda^{2n}$, and so forth. In particular, if $n = d = 3$, both C_λ^0 and C_λ^3 are fixed basins, C_λ^1 and C_λ^5 are mapped to C_λ^3, and C_λ^2 and C_λ^4 are mapped to C_λ^0.

Let $p_\lambda^j = \omega^j p_\lambda^0$, $q_\lambda^j = \omega^j q_\lambda^0$, and $u_\lambda^j = \omega^j u_\lambda^0$. Then both q_λ^j and u_λ^j lie on ∂C_λ^j. Also, p_λ^j lies in the interior of C_λ^j and is either periodic or preperiodic (see Figure 6).

For the other $n-2$ main cardioids of the principal Mandelbrot sets, we have a similar structure due to the $(n-1)$-fold symmetry in the parameter plane. More precisely, if ν is an $(n-1)^{\text{st}}$ root of unity, the orbits of the critical points of F_λ and $F_{\nu\lambda}$ behave symmetrically with respect to multiplication by some (fractional) power of ν, as was shown immediately following Symmetry Lemma 3. Consequently, the configuration of the basins for $F_{\nu\lambda}$ is similar to that of F_λ.

Recall that ∂B_λ and ∂T_λ are simple, closed curves. Since there are no critical points in $\partial B_\lambda \cap \partial T_\lambda$, these curves do not intersect. Let A_λ denote the closed annulus bounded by ∂B_λ and ∂T_λ. Let I_λ^j denote the closed set in A_λ that is contained in the region located between the open disks C_λ^j and C_λ^{j+1}. Note that the intersection of I_λ^j and I_λ^{j+1} is the pair of points q_λ^{j+1} and u_λ^{j+1}. Thus there are four points on the boundary of each I_λ^j that also lie on the boundary of another such set: a pair of points lies in $I_\lambda^j \cap I_\lambda^{j+1}$ and another pair in $I_\lambda^j \cap I_\lambda^{j-1}$. We call the points q_λ^j the outer junction points and the points u_λ^j the inner junction points (see Figure 6).

Proposition 2. F_λ maps each I_λ^j univalently (except at the junction points) over the region that is the complement of the three sets B_λ, $F_\lambda(C_\lambda^j)$, and $F_\lambda(C_\lambda^{j+1})$.

Proof: Since F_λ is conjugate to $z \mapsto z^n$ on ∂B_λ, the portion of ∂B_λ that
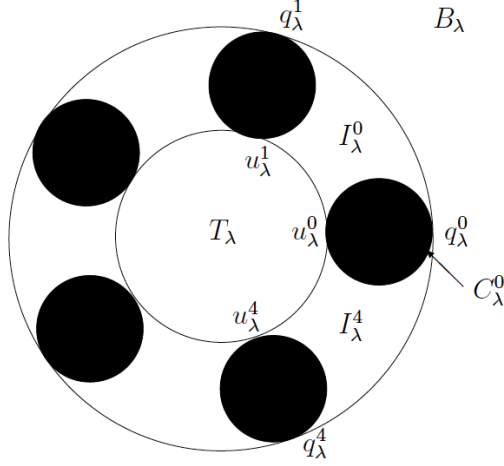
Figure 6: The regions I_λ^j if $n = 3$ and $d = 2$.

meets I_λ^j, i.e., the arc in ∂B_λ connecting q_λ^j to q_λ^{j+1}, is mapped to an arc in ∂B_λ that passes through exactly $n + 1$ outer junction points. Similarly, the portion of ∂T_λ that meets I_λ^j is mapped to the complementary arc in ∂B_λ. These two arcs meet at a pair of outer junction points in ∂B_λ. Also, the portion of the boundary of I_λ^j that meets ∂C_λ^j is mapped one-to-one onto the boundary of $F_\lambda(C_\lambda^j)$ except at the junction points. The junction points are both mapped to the same point. Similarly the other boundary of I_λ^j that lies in ∂C_λ^{j+1} is mapped onto $\partial F_\lambda(C_\lambda^{j+1})$. Therefore, the boundary of I_λ^j is mapped to the boundary of the three sets B_λ, $F_\lambda(C_\lambda^j)$, and $F_\lambda(C_\lambda^{j+1})$. Since there are no critical points in I_λ^j, the result follows. □

We call the two arcs in I_λ^j that lie in the boundaries of C_λ^j and C_λ^{j+1} the internal boundary components of I_λ^j. By Proposition 2, there must be a preimage of T_λ in each I_λ^j. Moreover, the boundary of this preimage must meet each internal boundary component of I_λ^j in exactly one point, namely the preimage of the inner junction points lying in the portions of the boundary of $F_\lambda(C_\lambda^j)$ and $F_\lambda(C_\lambda^{j+1})$ that lie in I_λ^j. Thus the preimage of T_λ in each I_λ^j is an open region whose boundary meets exactly one point in each of the boundaries of the connecting Fatou components that are adjacent to I_λ^j (see

13

Figure 7).

The preimage of T_λ separates I_λ^j into two pieces: an external piece that abuts ∂B_λ and an internal piece that abuts ∂T_λ. The external piece is mapped by F_λ over the portion of A_λ that stretches from $F_\lambda(C_\lambda^j)$ to $F_\lambda(C_\lambda^{j+1})$ in the counterclockwise direction. Since $F_\lambda(\omega z) = \omega^n F_\lambda(z)$, this region is mapped over exactly n of the I_λ^i and $n-1$ of the C_λ^i. Similarly, the internal piece is mapped over exactly d of the I_λ^i and $d-1$ of the C_λ^j. So each of I_λ^j can be further subdivided as shown in Figure 7. The portion of I_λ^j lying outside the preimage of T_λ has $n-1$ preimages of the connecting components, and the internal portion has $d-1$ such preimages. Between each preimage including C_λ^j and C_λ^{j+1}, there is a region that is mapped univalently onto one of the I_λ^k's. Hence there is a preimage of each of the sets just constructed in each of these smaller regions (see Figure 7).
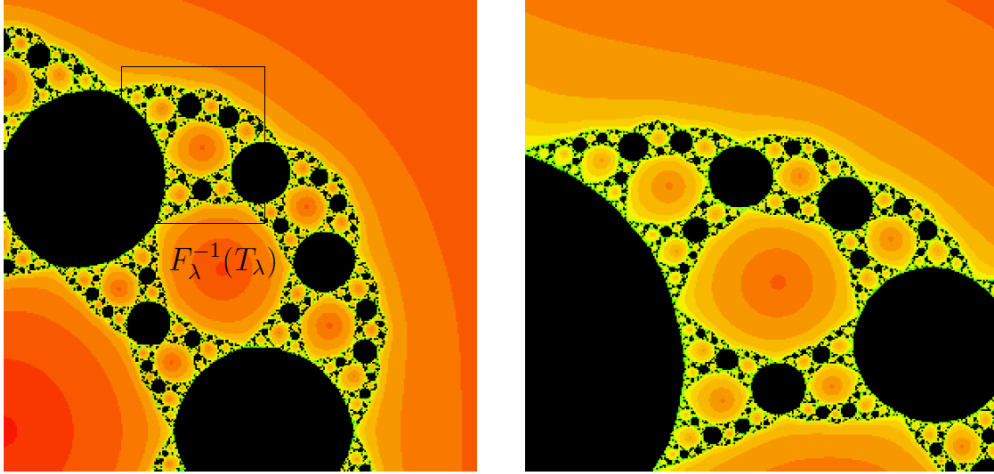

Figure 7: The regions I_λ^j if $n = 3$ and $d = 2$.

Continuing in this fashion, we always find the same picture in each region bounded by k^{th} and earlier preimages of T_λ and k^{th} and earlier preimages of the C_λ^j's. It is a central $(k+1)^{\text{st}}$ preimage of T_λ flanked by $n-1$ $(k+1)^{\text{st}}$ preimages of the connecting components on one side and $d-1$ other $(k+1)^{\text{st}}$ preimages on the other side.

14

However, this construction does not give the entire Julia set of F_λ. Indeed, the portion of the Julia set produced thus far contains only preimages of the boundaries of B_λ and the C_λ^j. None of these preimages contain any periodic points; the only periodic points here lie in ∂B_λ and ∂C_λ^j. So there must be more to the Julia set.

To complete the construction of the Julia set, note that each closed region I_λ^j is almost mapped univalently over the union of all of the I_λ^ks. The map is univalent except at the four junction points. One pair of junction points is mapped to an outer junction point in the image, and the other pair is mapped to a different outer junction point. We can use symbolic dynamics to identify each point in the Julia set. Let Σ denote the set of sequences $(s_0, s_1, s_2, \ldots)$ where each s_j is one of the integers $0, 1, \ldots, n + d - 1$. We identify each point in $J(F_\lambda)$ with a point in Σ by assigning to each $z \in J(F_\lambda)$ its itinerary $S(z) = (s_0, s_1, s_2, \ldots)$ where $s_k = j$ if $F_\lambda^k(z) \in I_\lambda^j$. However, infinitely many points are assigned to a pair of sequences. The points q_λ^j and u_λ^j each have a pair of sequences attached to them since these points reside in two of the I_λ^j's. For example, $S(q_\lambda^0) = (\overline{0}) = (\overline{n + d - 1})$ and $S(u_\lambda^0) = (0, \overline{n + d - 1}) = (n + d - 1, \overline{0})$. Similarly, any point that is eventually mapped onto a q_λ^j or a u_λ^j also has a pair of itineraries, e.g., the itineraries $(s_0, \ldots, s_k, 0, \overline{n + d - 1})$ and $(s_0, \ldots, s_k, n + d - 1, \overline{0})$ correspond to the same points.

We let Σ' denote the sequence space with the above identifications and endow Σ' with the quotient topology. Since each I_λ^j is mapped univalently (except at the junction points) over the union of the I_λ^k and the Julia set is contained in this union, standard arguments then show that the Julia set is homeomorphic to Σ'. The subsets Σ_j' of Σ' consisting of all sequences that start with the digit j correspond to points in $I_\lambda^j \cap J(F_\lambda)$, and they are homeomorphic to Σ_k'. It is important to note that the dynamics on these sets are not the same even though they are homeomorphic. We have described the topological structure of each $I_\lambda^j \cap J(F_\lambda)$, and this description implies Theorem 1 (see [2] for a similar argument).

3 Dynamical Invariants

In this section we prove Theorems 2 and 3. Let $\nu = \exp(2\pi i/(n-1))$. We show that two maps drawn from the main cardioids of different principal Mandelbrot sets are conjugate on their Julia sets if and only if the cardioids are located symmetrically under either the maps $z \mapsto \nu^{j(d+1)} z$ or $z \mapsto \nu^{j(d+1)} \overline{z}$ for some integer j.

We first observe that it suffices to prove this result for the special maps whose parameter is the *center* of these main cardioids. The set of critical points is invariant under the map, so the critical points are either periodic or preperiodic. The following proposition follows from the work of Mané, Sad, and Sullivan [10].

Proposition 3. *Suppose λ lies at the center of the main cardioid of one of the principal Mandelbrot sets and that μ lies in the same cardioid. Then F_λ and F_μ are quasiconformally conjugate on their Julia sets.*

Remark. It is not true that F_λ and F_μ are globally conjugate since F_λ has a superattracting cycle while the attracting cycle for F_μ need not be superattracting.

By Proposition 3, we need only consider parameters that lie at the centers of the main cardioids of the principal Mandelbrot sets. So for the remainder of this section, we assume that λ and μ are centers. Then $\mu = \nu^j \lambda$ for some $j \in \mathbb{Z}$. The proof of one direction of Theorem 2 is straightforward:

Proposition 4. *If $\mu = \nu^{j(d+1)} \lambda$ or $\mu = \nu^{j(d+1)} \overline{\lambda}$ for some integer j, then F_μ is conjugate to F_λ.*

Proof: Let $\mu = \nu^{j(d+1)} \lambda$, then

$$F_\mu(\nu^j z) = \nu^{jn} z^n + \frac{\lambda \nu^{j(d+1)}}{\nu^{jd} z^d} = \nu^j \left(z^n + \frac{\lambda}{z^d} \right) = \nu^j F_\lambda(z).$$

So F_λ is conjugate to F_μ via the linear map $z \mapsto \nu^j z$.

By Symmetry Lemma 1, F_λ and $F_{\overline{\lambda}}$ have conjugate dynamics. So if $\mu = \nu^{j(d+1)} \overline{\lambda}$, then F_μ is conjugate to $F_{\overline{\lambda}}$ and hence also to F_λ.

$\square$

From Proposition 4, we know that all centers whose parameters are of the form $\nu^k \lambda$ or $\nu^k \overline{\lambda}$ where $k = j(d+1) \bmod (n-1)$ have conjugate dynamics. That is, any two main cardioids that are located symmetrically with respect to either rotation by ν^{d+1} or complex conjugation have conjugate dynamics. Note that $\nu^{d+1} = \nu^{n-1} \nu^{d+1} = \nu^{n+d}$, so we can say that any two cardioids that are located symmetrically with respect to either rotation by ν^{n+d} or complex conjugation have conjugate dynamics.

Using basic facts about the greatest common divisor of two numbers, we can restate this relationship among the centers with conjugate dynamics in terms of the greatest common divisor g of $d+1$ and $n-1$. In fact, all centers whose parameters are of the form $\nu^k \lambda$ or $\nu^k \overline{\lambda}$ where k is an integer multiple of g have conjugate dynamics.

Now we show that these symmetrically located centers are the only centers with conjugate dynamics. First we define the minimum rotation number for parameters in the main cardioids of the principal Mandelbrot sets. For each such parameter we have $n+d$ connecting components C_λ^j with j defined mod $n+d$, and the C_λ^j are ordered in the counterclockwise direction as j increases. Each of these connecting components is mapped two-to-one onto another such component since each contains a unique critical point (see Figure 6).

Suppose $F_\lambda(C_\lambda^j) = C_\lambda^k$. We define the rotation number ρ_j of C_λ^j to be the value of $k-j$ that is closest to 0 for any $k \bmod n+d$. Note that it is possible for k to be negative (see Figure 8). For example, if $F_\lambda(C_\lambda^0) = C_\lambda^{n+d-1}$, then the rotation number of C_λ^0 would be -1 since $C_\lambda^{n+d-1} = C_\lambda^{-1}$. We say that C_λ^j is rotated through $k-j$ components if $\rho_j = k$. We then define the *minimum rotation number* $\rho(\lambda)$ for F_λ to be the minimum value of $|\rho_j|$ over all j. For example, if F_λ has an attracting fixed point in some C_λ^j, $\rho(\lambda) = 0$. If there is no such attracting fixed point, then $\rho(\lambda) > 0$.

Proposition 5. *Let λ and μ be centers of main cardioids of principal Mandelbrot sets. Then F_λ is conjugate to F_μ if and only if $\rho(\lambda) = \rho(\mu)$. Equivalently, $\mu = \nu^k \lambda$ or $\mu = \nu^k \overline{\lambda}$ where $k = j(d+1) \bmod (n-1)$ for some integer j. The conjugating map is either a rotation about the origin or a rotation*
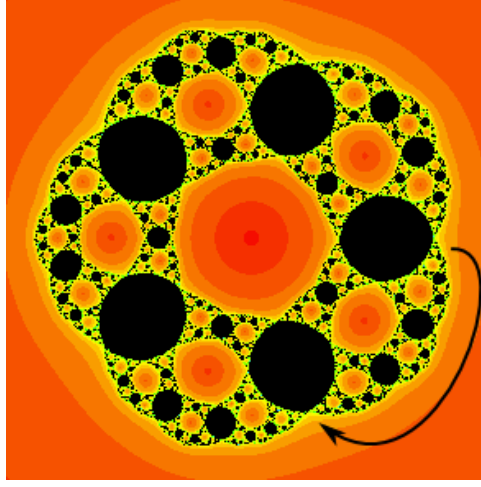
17

Figure 8: A C_λ^j with $\rho_j = -1$.

followed by complex conjugation.

Proof: First suppose that two such centers λ and μ have different minimum rotation numbers. Then F_λ and F_μ cannot be conjugate on their Julia sets. To see why, recall that the connecting components each touch ∂B_λ at exactly one point. Now ∂B_λ must be sent to itself by any conjugacy between F_λ and F_μ since this set is the only invariant subset of the Julia set that touches the boundaries of all of the connecting components. Thus the ordering of the C_λ^j is either preserved or reversed by the conjugacy, i.e., either the conjugacy rotates the connecting components in one direction or the other, or the conjugacy first applies complex conjugation followed by some rotation. In either case, if the minimum rotation numbers of F_λ and F_μ are different, then such a conjugacy cannot exist.

To prove the converse, we consider the set of critical points, $c_\lambda^0, \ldots, c_\lambda^{n+d-1}$, of F_λ where λ is the center of a main cardioid of a principal Mandelbrot set. The point c_λ^j is the unique critical point that lies in the connecting component C_λ^j. We note that this set of critical points is invariant under F_λ.

Suppose F_λ and F_μ have the same minimum rotation number m. By assumption, there is at least one critical point c_λ^j for F_λ for which either

18

$F_\lambda(c_\lambda^j) = c_\lambda^{j+m} = \omega^m c_\lambda^j$ or $F_\lambda(c_\lambda^j) = c_\lambda^{j-m} = \omega^{-m} c_\lambda^j$. (Recall that $\omega^{n+d} = 1$.) There is also a critical point c_μ^i for F_μ for which either $F_\mu(c_\mu^i) = c_\mu^{i+m} = \omega^m c_\mu^i$ or $F_\mu(c_\mu^i) = c_\mu^{i-m} = \omega^{-m} c_\mu^i$.

We consider the first case for λ and μ, i.e., where the rotation numbers m for both critical points are positive. Since $\mu = \nu^k \lambda$ for some k, F_μ is conjugate to the map $z \mapsto \omega^k F_\lambda(z)$ by the rotation $z \mapsto \eta^k z$ where

$$\eta = \exp(2\pi i/((n+d)(n-1)))$$

(see the paragraphs that follow Symmetry Lemma 3). So there must be a critical point for $\omega^k F_\lambda$ that corresponds to c_μ^i and that is also rotated by ω^m when $\omega^k F_\lambda$ is applied to it. But any critical point of $\omega^k F_\lambda$ must also be a critical point for F_λ. Suppose that $\omega^\ell c_\lambda^j$ is the critical point for $\omega^k F_\lambda$ that corresponds to c_μ^i. Then we have

$$\omega^k F_\lambda(\omega^\ell c_\lambda^j) = \omega^m \omega^\ell c_\lambda^j = \omega^\ell \omega^m c_\lambda^j = \omega^\ell F_\lambda(c_\lambda^j).$$

But

$$\omega^k F_\lambda(\omega^\ell c_\lambda^j) = \omega^{k+\ell n} F_\lambda(c_\lambda^j).$$

Therefore we have $\ell = k + \ell n \bmod (n+d)$.

Consequently, $\omega^\ell F_\lambda(z) = \omega^{k+\ell n} F_\lambda(z)$, and using Symmetry Lemma 2, we obtain

$$\omega^\ell F_\lambda(z) = \omega^k F_\lambda(\omega^\ell z)$$

for all $z \in \mathbb{C}$. So F_λ is conjugate to $\omega^k F_\lambda$ via the map $z \mapsto \omega^\ell z$. Therefore F_λ is also conjugate to F_μ via a linear map of the form $z \mapsto \eta \omega^\ell z$ and $\mu = \nu^k \lambda$ where $k = j(d+1) \bmod (n-1)$.

The proof for the case where both rotation numbers m are negative is exactly the same.

To prove the second case, the case where the rotations go in opposite directions, we simply conjugate F_μ to $F_{\overline{\mu}}$ by complex conjugation and then invoke the first case. $\square$

As a consequence of Propositions 3 and 5, this result extends to all parameters in the main cardioids of any of the principal Mandelbrot sets.

Corollary. *Let λ and μ be any parameters drawn from the main cardioids of any two prinicpal Mandelbrot sets. Then F_λ and F_μ are conjugate on their Julia sets if and only if $\rho(\lambda) = \rho(\mu)$.*

Now we can determine exactly which main cardioids of the principal Mandelbrot sets have conjugate dynamics and the precise number of different conjugacy classes. Let $\mathcal{M}_0$ denote the main cardioid of the principal Mandelbrot set that intersects the positive real axis, and denote the remaining main cardioids of principal Mandelbrot sets by $\mathcal{M}_j$ where the ordering is in the counterclockwise direction. We write $\mathcal{M}_j \equiv \mathcal{M}_k$ if the parameters at the centers of $\mathcal{M}_j$ and $\mathcal{M}_k$ have conjugate dynamics. Let g be the greatest common divisor of $n - 1$ and $d + 1$. As we proved in this section, the principal Mandelbrot sets with dynamics conjugate to the dynamics of $\mathcal{M}_k$ are those obtained by successive rotations in the parameter plane by $z \mapsto \nu^{jg}z$ or by these rotations followed by complex conjugation. In particular, we have $\mathcal{M}_0 \equiv \mathcal{M}_{jg}$ for all integers j.

Theorem. *If the greatest common divisor g is even, there are $1 + g/2$ different conjugacy classes among the $\mathcal{M}_j$. If g is odd, there are $(g+1)/2$ distinct such conjugacy classes.*

Proof: First suppose that $g = 1$. Then all maps drawn from the $\mathcal{M}_j$ have conjugate dynamics, so we have $1 = (g + 1)/2$ conjugacy classes.

Now suppose $g > 1$. We claim that $\mathcal{M}_k \not\equiv \mathcal{M}_0$ for any k with $0 < k < g$. If not, then maps at the centers of $\mathcal{M}_0$ and some $\mathcal{M}_k$ would be conjugate by $z \mapsto \overline{z}$ followed possibly by a rotation. But then $\mathcal{M}_k \equiv \mathcal{M}_{-k}$ via $z \mapsto \overline{z}$. Also, $\mathcal{M}_g \equiv \mathcal{M}_{-g}$ by $z \mapsto \overline{z}$. Therefore we have $\mathcal{M}_{-g} \equiv \mathcal{M}_{-k}$ by a rotation, which would imply that the greatest common divisor is smaller than g. So none of the centers of the $\mathcal{M}_k$ with $0 < k < g$ have dynamics conjugate to the center of $\mathcal{M}_0$.

If g is even, we consider $\mathcal{M}_k$ where $0 < k < g/2$. We have $\mathcal{M}_k \equiv \mathcal{M}_{-k}$ by complex conjugation. Moreover $\mathcal{M}_{-k} \equiv \mathcal{M}_{g-k}$ since these sets are symmetric under the rotation $z \mapsto \nu^g z$, so $\mathcal{M}_k \equiv \mathcal{M}_{g-k}$. On the other hand, we cannot have $\mathcal{M}_k \equiv \mathcal{M}_j$ for any other j with $0 < j < g$ via rotation

20

by $z \mapsto \nu^g z$ or by complex conjugation coupled with a rotation, so the principal Mandelbrot sets with dynamics conjugate to those in $\mathcal{M}_k$ are just the rotations of $\mathcal{M}_k$ together with their complex conjugates. The number of such conjugacy classes is $g/2 - 1$. We have $\mathcal{M}_{g/2} \equiv \mathcal{M}_{-g/2}$ by the rotation $z \mapsto \nu^{-g} z$ as well as by complex conjugation. So $\mathcal{M}_{g/2}$ lies in a conjugacy class that is distinct from the classes of the $\mathcal{M}_k$ with $0 \leq k \leq g/2$. The conjugacy class of $\mathcal{M}_0$ has not yet been counted. Combining all of these classes, we obtain a total of $1 + g/2$ distinct conjugacy classes.

If g is odd, we count in exactly the same way except that we do not have a conjugacy class that corresponds to $\mathcal{M}_{g/2}$ in this case.

$\square$

See Figure 9 for the three orbit diagrams that arise if $n = 13$ and $d = 7$. In Figure 10, we consider the case where $n = 11$ and $d = 4$, and group the Mandelbrot sets whose centers have conjugate dynamics.
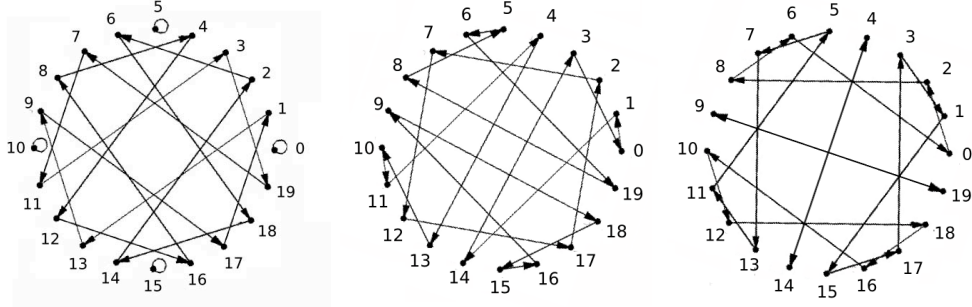

Figure 9: If $n = 13$ and $d = 7$, then $g = 4$, and consequently, there are three conjugacy classes. This figure contains one orbit diagram for each of the three classes.

4 A Group Action

Since the conjugacies among the $\mathcal{M}_k$ arise from reflective and rotational symmetries, we can count the number of conjugacy classes by viewing them
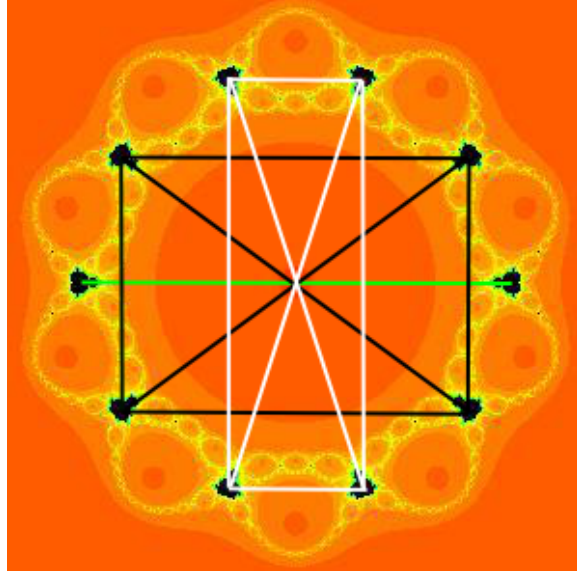
Figure 10: If $n = 11$ and $d = 4$, then $g = 5$, and consequently, there are three conjugacy classes. The parameters with conjugate dynamics are connected by segments of the same color, e.g., the four Mandelbrot sets connected by white segments all have conjugate dynamics.

as orbits of the action of a dihedral group on the set $\{\mathcal{M}_k\}$, viewed as the vertices of a regular $(n-1)$-gon.

Let $a = (n-1)/g$. We claim that the natural group that produces these orbits is D_{2a}, the group of symmetries of a regular a-gon. Let s be the generator of D_{2a} corresponding to reflection and r be the generator corresponding to rotation. We define the action of D_{2a} on $\{\mathcal{M}_k\}$ by

$$
\begin{aligned}
s\mathcal{M}_k &= \mathcal{M}_{-k \bmod n-1} \\
r\mathcal{M}_k &= \mathcal{M}_{k+g \bmod n-1}
\end{aligned}
$$

These rules produce a well-defined D_{2a} action, and since the actions on $\{\mathcal{M}_k\}$ by s and r are exactly complex conjugation and rotation by $z \mapsto \nu^g z$, respectively, the orbits of this action correspond exactly to the conjugacy classes among the $\mathcal{M}_k$.

By Burnside's Lemma, the number of orbits is

$$\frac{1}{|D_{2a}|} \sum_{x \in D_{2a}} |\text{fix}(x)|$$

where $\text{fix}(x) = \{\mathcal{M}_i \in \{\mathcal{M}_k\} : x\mathcal{M}_i = \mathcal{M}_i\}$.

The group D_{2a} has $2a$ elements, and each can be written as r^j or sr^j with $0 \le j < a$. The identity fixes all $n - 1$ elements of $\{\mathcal{M}_k\}$, and r^j fixes none for $0 < j < a$. Thus the number of orbits is

$$\frac{1}{2a} \left(n - 1 + \sum_{j=0}^{a-1} |\text{fix}(sr^j)| \right)$$

An element of the form sr^j rotates each $\mathcal{M}_k$ by $z \mapsto \nu^{jg} z$ and then reflects it about the real axis. Equivalently, it reflects the $\mathcal{M}_k$ through some axis of symmetry of the set viewed as a regular $(n-1)$-gon. Thus, if $n - 1$ is odd, every such axis passes through exactly one of the $\mathcal{M}_k$, and thus $|\text{fix}(sr^j)| = 1$ for all j. The formula above then shows the number of conjugacy classes is $(n - 1 + a)/2a = (g + 1)/2$.

If $n - 1$ is even, half of the axes of symmetry pass through two of the $\mathcal{M}_k$, and half pass through none. Thus sr^j fixes either two or zero of the $\mathcal{M}_k$. There exists a j such that sr^j fixes none of the $\mathcal{M}_k$ if and only if there is some i such that $sr^j \mathcal{M}_i = \mathcal{M}_{i+1 \bmod n-1}$, i.e., the axis of reflection passes between $\mathcal{M}_i$ and $\mathcal{M}_{i+1 \bmod n-1}$ for some i. For such an i, $r^j \mathcal{M}_i = s^{-1} \mathcal{M}_{i+1 \bmod n-1} = \mathcal{M}_{-i-1 \bmod n-1}$ which equals $\mathcal{M}_{i+jg \bmod n-1}$ by the definition of the action of r. Thus $-i - 1 \equiv i + jg \bmod n - 1$, and hence, $2i + jg + 1 \equiv 0 \bmod n - 1$. If either j or g is even, this equality is impossible since $n - 1$ is even, and therefore, sr^j must fix two of the $\mathcal{M}_k$. If j and g are both odd, however, any i with $i \equiv (-jg - 1)/2 \bmod n - 1$ satisfies the congruence, and thus sr^j fixes none of the $\mathcal{M}_k$.

Therefore, if $n - 1$ and g are even, then $|\text{fix}(sr^j)| = 2$ for all j, and the number of conjugacy classes is $(n - 1 + 2a)/2a = 1 + g/2$. If $n - 1$ is even and g is odd, $|\text{fix}(sr^j)|$ equals 2 if j is even, and 0 if j is odd. Hence, there are $(n - 1 + a)/2a = (g + 1)/2$ conjugacy classes.

Finally, if $n-1$ is odd, g must be odd, so the possible cases really depend only on the parity of g and not of $n-1$. Hence, the number of conjugacy classes is $(g+1)/2$ if g is odd and $1+g/2$ if g is even.

References

[1] Blanchard, P., Devaney, R. L., Look, D. M., Seal, P., and Shapiro, Y. Sierpiński Curve Julia Sets and Singular Perturbations of Complex Polynomials. *Ergodic Theory and Dynamical Systems*, **25** (2005), 1047–1055.

[2] Çilingir, F., Devaney, R. L., and Russell, E. D. Extending external rays throughout the Julia sets of rational maps. *Journal of Fixed Point Theory and Applications*, appeared online March 10, 2011.

[3] Devaney, R. L. and Look, D. M. Buried Sierpiński Curve Julia Sets. *Discrete and Continuous Dynamical Systems* **13** (2005), 1035–1046.

[4] Devaney, R. L., Look, D. M. A Criterion for Sierpiński Curve Julia Sets. *Topology Proceedings* **30** (2006), 163–179.

[5] Devaney, R. L., Look, D. M., and Uminsky, D. The Escape Trichotomy for Singularly Perturbed Rational Maps. *Indiana University Mathematics Journal* **54** (2005), 1621–1634.

[6] Devaney, R. L. and Pilgrim, K. Dynamic Classification of Escape Time Sierpinski Curve Julia Sets. *Fundamenta Mathematicae* **202** (2009), 181–198.

[7] Devaney, R. L. Cantor Necklaces and Structurally Unstable Sierpiński Curve Julia Sets for Rational Maps. *Qualitative Theory of Dynamical Systems* **5** (2004), 337–359.

[8] Devaney, R. L. Baby Mandelbrot Sets Adorned with Halos in Families of Rational Maps. In *Complex Dynamics: Twenty-Five Years after the Appearance of the Mandelbrot Set.* American Math Society, Contemporary Math **396** (2006), 37–50.

[9] Devaney, R. L. A Myriad of Sierpiński Curve Julia Sets. In *Difference Equations, Special Functions, and Orthogonal Polynomials.* World Scientific, 2007, 131–148.

[10] Mañé, R., Sad, P., and Sullivan, D., On the dynamics of rational maps. *Annales Scientifiques de l'École Normale Supérieure. Quatrième Série* **16**, 1983, 193–217.

[11] McMullen, C. Automorphisms of Rational Maps. *Holomorphic Functions and Moduli*. Vol. 1. Math. Sci. Res. Inst. Publ. **10**. Springer, New York, 1988.

[12] McMullen, C. The Classification of Conformal Dynamical Systems. *Current Developments in Mathematics*. International Press, Cambridge, MA, (1995) 323–360.

[13] Milnor, J. Dynamics in One Complex Variable, 3ed, Princeton University Press, 2006.

[14] Milnor, J. and Tan Lei. A "Sierpiński Carpet" as Julia Set. Appendix F in Geometry and Dynamics of Quadratic Rational Maps. *Experiment. Math.* **2** (1993), 37–83.

[15] Whyburn, G. T. Topological characterization of the Sierpiński curve, *Fund. Math.* **45** (1958), 320–324.